

A routing framework for energy harvesting wireless nanosensor networks in the Terahertz Band

Massimiliano Pierobon · Josep Miquel Jornet ·
Nadine Akkari · Suleiman Almasri ·
Ian F. Akyildiz

© Springer Science+Business Media New York 2013

Abstract Wireless NanoSensor Networks (WNSNs) will allow novel intelligent nanomaterial-based sensors, or nanosensors, to detect new types of events at the nanoscale in a distributed fashion over extended areas. Two main characteristics are expected to guide the design of WNSNs architectures and protocols, namely, their Terahertz Band wireless communication and their nanoscale energy harvesting process. In this paper, a routing framework for WNSNs is proposed to optimize the use of the harvested energy to guarantee the perpetual operation of the WNSN while, at the same time, increasing the overall network throughput. The proposed routing framework, which is based on a previously proposed medium access control protocol for the joint throughput and lifetime optimization

in WNSNs, uses a hierarchical cluster-based architecture that offloads the network operation complexity from the individual nanosensors towards the cluster heads, or nano-controllers. This framework is based on the evaluation of the probability of saving energy through a multi-hop transmission, the tuning of the transmission power of each nanosensor for throughput and hop distance optimization, and the selection of the next hop nanosensor on the basis of their available energy and current load. The performance of this framework is also numerically evaluated in terms of energy, capacity, and delay, and compared to that of the single-hop communication for the same WNSN scenario. The results show how the energy per bit consumption and the achievable throughput can be jointly maximized by exploiting the peculiarities of this networking paradigm.

M. Pierobon (✉)
Department of Computer Science and Engineering, University of
Nebraska-Lincoln, Lincoln, NE 68588, USA
e-mail: maxp@unl.edu; pierobon@cse.unl.edu

J. M. Jornet
Department of Electrical Engineering, University at Buffalo, The
State University of New York, Buffalo, NY 14260, USA
e-mail: jmjornet@buffalo.edu

N. Akkari · S. Almasri · I. F. Akyildiz
Faculty of Computing and Information Technology, King
Abdulaziz University, Jeddha, Saudi Arabia
e-mail: nakkari@kau.edu.sa

S. Almasri
e-mail: smalmasri@kau.edu.sa

I. F. Akyildiz
e-mail: ian@ece.gatech.edu

I. F. Akyildiz
Broadband Wireless Networking Laboratory, School of
Electrical and Computer Engineering, Georgia Institute of
Technology, Atlanta, GA 30332, USA

Keywords Nanosensors · Nanonetworks · Routing ·
Terahertz Band · Energy harvesting

1 Introduction

Among the more promising research fields of today, nanotechnology is enabling the manipulation of matter at an atomic and molecular scale, from one to a hundred nanometers. One of the goals of nanotechnology is to engineer functional systems based on the unique phenomena and properties of matter at the nanoscale [5]. Currently, a great research effort is spent in the attempt to realize nanoscale machines, also called molecular machines or nanomachines, defined by Drexel [6] as “mechanical devices that perform useful functions using components of nanometer-scale and defined molecular structure”. More specifically, nanosensors [1] are nanomachines expected to have the ability to sense, compute, manage their energy,

and interconnect into networks, termed Wireless Nano-Sensor Networks (WNSNs), to overcome their individual limitations and benefit from collaborative efforts. WNSNs will take advantage of novel nanomaterial-based sensing processes to detect new types of events at the nanoscale, and they are expected to enable advanced applications of nanotechnology in the biomedical field (e.g., intrabody health monitoring and drug delivery systems), environmental control (e.g., agriculture plague and air pollution control), and defense and military technology (e.g., surveillance against new types of biological and chemical attacks at the nanoscale).

Among the many peculiarities of nanosensors, two main characteristics, combined with their limited computational resources [14], are expected to guide the design of WNSNs architectures and protocols, namely, their wireless communication technology and their energy harvesting process. The limited size of nanosensors is notoriously excluding the possibility of designing on-board classical antennas, which would radiate only at extraordinary high frequencies, up to hundreds of THz, infeasible given the limited energy resources available. Nanomaterial-based antennas, in particular graphene-based antennas [10, 11, 16, 17] and nano-transceivers [4, 11, 15], are proposed as a solution to the aforementioned problem, since the properties of graphene allow them to radiate in the Terahertz Band, within 0.1 and 10 THz, while having a form factor suitable to be integrated into nanosensors. Very high propagation losses and a very large available bandwidth are the main Terahertz Band communication characteristics [8, 13] which have to be taken into account to develop efficient WNSNs architectures and protocols, while jointly taking into account the limited nanosensor resources in terms of computational power and energy.

An energy harvesting process is required by nanosensors to cope with the limited size and flexibility of their energy storage, which is realized by means of nano-batteries. In this direction, energy harvesting processes at the nanoscale have been recently proposed [3, 7, 19], which convert several different forms of energy, e.g., vibrational, fluidic, electromagnetic, or acoustic, into electrical energy. The peculiarities of these nanoscale energy harvesting processes combined with the limited energy storage of the nanosensors result in temporal fluctuations of the available energy of each nanosensor, which have to be taken into account when designing WNSNs architectures and protocols. In this direction, WNSNs have the potential to achieve an infinite lifetime and perpetual operations if carefully adapted to these peculiarities, as detailed in [18].

The very high density of nodes expected for a WNSNs, combined with the very high propagation losses of the Terahertz Band channel and the need to efficiently meet the conditions for perpetual network operations, require the

development of novel routing protocols for multi-hop communication in WNSNs. To the best of our knowledge, there are no routing protocols for WNSNs. In addition, previous work on energy efficient routing in WSNs is not directly applicable to WNSNs, since the peculiarities of the Terahertz Band communication [8], in particular the very unique distance-dependent behavior of the available bandwidth and the power control techniques that can be employed to reach the optimal transmission rate, are not taken into account. Moreover, other work focused on routing in WSN with energy harvesting nodes does not capture the particular characteristics of the energy harvesting processes at the nanoscale [9], in particular the collection of vibrational energy through piezoelectric nanogenerators. As a consequence, novel solutions for the design of a routing scheme, where the peculiarities of the wireless communication in a WNSN are combined with the energy-efficient management of the information routing scheme, are needed.

In this paper, we devise a novel routing framework based on the peculiarities of the WNSNs, both in term of Terahertz Band communication and nano-scale energy harvesting. First, this routing framework is based on a hierarchical cluster-based architecture where the WNSN is partitioned into clusters. Within each cluster, a nano-controller, which is a nano device with more advanced capabilities than a nanosensor, coordinates the nanosensors and gathers the data they communicate [1]. This hierarchical cluster-based architecture is specifically devised to manage most of the complexity of any network protocol or algorithm at the nano-controller, and to cope with the limited resources of the nanosensors. Moreover, since the communication within the nanosensor network involves high-bit-rate transmissions in the Terahertz Band, the nano-controller is also responsible to guarantee the necessary synchronization at the physical layer. To reach this objective, our routing framework stems from the MAC protocol recently proposed in [18], where a joint throughput and lifetime scheduling is performed by the nano-controller on top of a Time Division Multiple Access TDMA framework within each cluster. In our routing framework, we specialize this throughput and lifetime scheduling to the multi-hop case, where a joint management of the direct communication from the nanosensors to the nano-controller and the multi-hop communication among nanosensors is performed, as detailed in Sect. 2.2.

Second, our routing framework is based on the evaluation of the probability of saving energy by initiating a multi-hop communication route from a source nanosensor compared to a direct transmission from the source nanosensor to the nano-controller. This evaluation is executed at the nano-controller, which is expected to make a decision toward multi-hop or direct communication on the basis of

the probability value. This procedure allows to initiate a multi-hop communication only when there is a sufficient probability of saving energy, which would finally result in an increase of the overall throughput of the network, as explained in Sect. 2.3

Third, in case of multi-hop communication, the nano-controller is expected to optimize the distance of the next hop through a control on the transmission power of the source nanosensor. This transmission power is adapted to the Critical Neighbor Range (CNR) parameter, defined in Sect. 2.4 as the optimal distance at which the next hop should be located from the source nanosensor to achieve the best trade-off between the throughput and the distance from the receiving neighbor node that guarantees a pre-defined received SNR value, while at the same time satisfying the condition for infinite network lifetime.

Finally, the selection of the next hop is operated in a distributed fashion, where each nanosensor sets its likelihood to be elected as next hop depending on the load in its retransmission buffer, the level of its stored energy, its closeness to the CNR, and its relative location with respect to the source nanosensor and the nano-controller, as detailed in Sect. 2.5 This procedure allows a balance in the use of the energy and computational resources in each cluster of the WNSN, while allowing the optimization of the throughput and guaranteeing the perpetual operation of the network.

The rest of the paper is organized as follows. The proposed routing framework is detailed in Sect. 2 Numerical results are included in Sect. 3, where a performance evaluation is conducted through simulations by comparing the proposed routing framework with a more basic single-hop communication. Finally, in Sect. 4 we conclude the paper.

2 WNSN routing framework

The objective of the routing framework is to provide the nanosensor network with a procedure to save the average energy harvested from the environment by the nanosensors and increase the overall throughput in the transmission of information from the nanosensors to the nano-controller. The routing decision framework is built on top of the Medium Access Control (MAC) protocol introduced in our previous work in [18], where a throughput-and-lifetime optimal scheduling was designed to manage a variable-length time slot assignment to the nanosensor for their direct transmission of information to the nano-controller. In this paper, we enhance this protocol by introducing the capability for each nanosensor to relay information coming from other nanosensors, thus enabling a multi-hop transmission of information from a nanosensor to the nano-controller. In Sect. 2.1, we introduce the nanosensor deployment model, while in Sect. 2.2 we describe the main

steps of the multi-hop decision algorithm involving each nanosensor willing to transmit information and the nano-controller. In Sects. 2.3, 2.4, 2.5, and 2.6, the main elements of the routing framework, namely, the computation of the probability of energy saving and the CNR, and the management of the random back-off time and the optimal scheduling of the nanosensor transmissions in the sub-frames, are analytically detailed. The most frequently used parameters in this section are reported in Table 1 by following the order of their appearance in the text.

2.1 Nanosensor deployment

The nanosensors are assumed to be deployed in the 2-dimensional space occupied by a WNSN cluster according to a spatial homogeneous Poisson counting process whose rate is equal to the nanosensor density ρ defined in Table 1. For this, the probability of having a count of k nanosensors in an area of value S within the WNSN cluster is expressed as follows:

$$P(k \text{ nanosensors in } S) = \frac{[\rho S]^k e^{-\rho S}}{k!}. \quad (1)$$

2.2 Multi-hop decision algorithm

The multi-hop decision algorithm is executed in the wireless nanosensor network every time a nanosensor n is willing to transmit data. With reference to [18], the communication between nanosensors and the nano-controller follows a dynamic Time Division Multiple Access (TDMA) scheduling, where a time frame structure is divided into four fixed-length sub-frames: DownLink (DL), UpLink (UL), MultiHop (MH), and RandomAccess (RA). The DL sub-frame is used by the nano-controller to send commands to the nanosensors, the UL subframe is used by nanosensors to send data to the nano-controller by using transmission timeslots assigned by the nano-controller, the MH sub-frame is used by nanosensors to exchange data with each other in an ad-hoc fashion by using time slots assigned by the nano-controller, and the RA sub-frame is used for communication of the willingness to transmit data from nanosensors to the nano-controller.

The routing decision algorithm involves the following steps, as summarized through the block scheme in Fig. 1:

1. A nanosensor n sends to the nano-controller a request to transmit data, which specifies the amount of information it needs to transmit P_n defined in Table 1. This communication takes place in the RA subframe and it is directed only to the nano-controller.
2. Upon receiving the request to transmit data from a nanosensor n , the nano-controller estimates the distance z_n between itself and the nanosensor n , and from

Table 1 Table of the most frequently used parameters in Sect. 2

Parameter	Definition
ρ	Nanosensor density in number of nanosensors per unit area
P_n	Amount of information the nanosensor n needs to transmit in number of packets
$P_{ES}(n)$	Probability of energy savings by multi-hop transmission for the nanosensor n
CNR_n	Critical Neighborhood Range for the nanosensor n
RTP_n	Required Transmission Power for the nanosensor n
$T_{B-O}(n, k)$	Random back-off time for the nanosensor k upon completion of the reception of the data transmission from the nanosensor n
$ACK(n, m)$	Acknowledgement for the nanosensor k upon completion of the random back-off time $T_{B-O}(n, k)$
$E_{bit}(l)$	Energy per bit to transmit in a single hop at a distance l
x_n	Distance between the node n and a random neighbor
y_n	Distance between the random neighbor of the nanosensor n and the nano-controller
z_n	Distance between the node n and the nano-controller
Φ	Angle between the line connecting the nanosensor n and the nano-controller and the line connecting the nanosensor n and its random neighbor
$\hat{E}_{bit}(x_n, \Phi)$	Average energy per bit from the random neighbor of the nanosensor n to the nano-controller
$S(z_n)$	Area spanned by all the possible values for the coordinates of a neighbor nanosensor in the plane defined by the angle between the line connecting the nanosensor n and the nano-controller and the line connecting the nanosensor n and the neighbor, which satisfy the inequality in (4)
SNR	Signal-to-Noise Ratio experienced by a receiver nanosensor
$P(l)$	Transmission power spent at a nanosensor to transmit in a single hop and guarantee a constant SNR at receiver placed at distance l
$C(l)$	Maximum data rate at which a nanosensor can transmit at a distance l while guaranteeing a predefined received SNR value
f_0	
c	
N_0	
E_r	Energy spent at the nanosensor to receive one bit, which is a constant parameter within the scope of this paper
$\Lambda(l)$	Maximum data rate at which a nanosensor can transmit at a distance l while guaranteeing a predefined received SNR value and infinite network lifetime
λ_{harv}	Energy harvesting rate for a nanosensor
$\lambda_{con}(l)$	Energy consumption rate for a nanosensor during transmission at a distance l
D_n	Size in bits of the incoming data from the nanosensor n
$e_m(t)$	Energy stored in the nanosensor m at time t is sufficient to complete the reception of the data from a nanosensor n
$RSSI(n, n - c)$	Received Signal Strength Indicator received at the nanosensor n upon a transmission from the nano-controller $n - c$
T_i	Minimum transmission period per packet for each nanosensor
N_{bits}	Number of bits in a packet

the knowledge of the nanosensors density ρ it computes the value of the probability $P_{ES}(n)$ of energy savings by multi-hop transmission for the nanosensor n , as explained in Sect. 2.3, through the expressions in (17), (19), and (6), respectively.

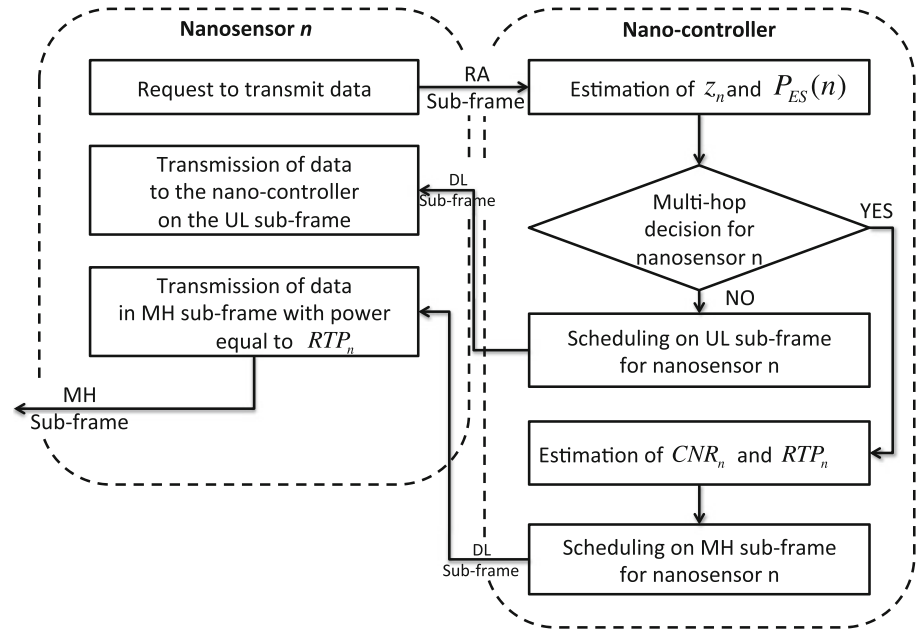
3. The nano-controller makes the decision for the nanosensor n to go either for a multi-hop transmission or for a single-hop transmission on the basis of the value of

the realization of a random variable with a Bernoulli distribution [12] having success probability equal to the probability $P_{ES}(n)$ of energy savings. This is expressed as follows:

$$\Pr\{n \text{ Multi-hop}\} = 1 - \Pr\{n \text{ Single-hop}\} = P_{ES}(n), \quad (2)$$

4. In case of a single-hop transmission decision for the nanosensor n , the nano-controller performs a scheduling

Fig. 1 Block Scheme of the multi-hop decision algorithm involving a nanosensor n and the nano-controller



on the UL sub-frame, as described in Sect. 2.6, where the nanosensor n is dynamically assigned variable-length time slots in the UL sub-frame on the basis of the communicated amount of information P_n it needs to transmit. The result of the scheduling is communicated from the nano-controller to the nanosensor n by using the DL sub-frame, and subsequently the data is transmitted directly from the nanosensor n to the nano-controller.

5. In case of multi-hop transmission decision for the nanosensor n , the following additional steps are performed:
 - The nano-controller computes for the nanosensor n the Critical Neighborhood Range CNR_n , which corresponds to the optimal distance at which the next hop should be located from the nanosensor n to achieve the best trade-off between the throughput and the distance from the receiving neighbor node that guarantees a predefined received SNR value, while at the same time satisfying the condition for infinite network lifetime. From the value of the CNR_n , the nano-controller computes the value of the Required Transmission Power RTP_n which the nanosensor n should use to achieve a predefined value for the received SNR at a receiver placed at a distance equal to CNR_n . The computations of CNR_n and RTP_n are detailed in Sect. 2.4 Moreover, the nano-controller, by applying the scheduling framework described in Sect. 2.6, assigns to the nanosensor n variable-length time slots within the MH sub-frame on the basis of the communicated amount of information P_n it needs to transmit, and communicates this information and the

value of the CNR_n to the nanosensor n by using the DL sub-frame.

- Upon reception of the information from the nano-controller transmitted in the DL sub-frame, the nanosensor n transmits its data in the MH sub-frame by using a transmission power equal to RTP_n and the time slots communicated by the nano-controller.
- Each nanosensor k receiving the data from the nanosensor n , upon completion of the reception of the data transmission, waits for a random back-off time $T_{B-O}(n, k)$. If a nanosensor m does not overhear in the RA sub-frame an Acknowledgement $ACK(n, k)$ message, where $k \neq m$, then it broadcasts an $ACK(n, m)$ in the RA sub-frame. The value of the back-off time $T_{B-O}(n, k)$ whose computation is detailed in Sect. 2.5 allows the nanosensors which are located farther from the nanosensor n , but closer to the CNR_n , to be more likely selected as the next hop for the transmission of the data coming from the nanosensor n .
- Upon completion of the reception of the data coming from the nanosensor n , the wireless nanosensor network repeats the aforementioned steps from Step 1 this time for the next hop nanosensor m , which becomes the new source node.

2.3 Probability of energy savings by multi-hop transmission

The probability $P_{ES}(n)$ of energy savings by multi-hop transmission for the nanosensor n is defined as the

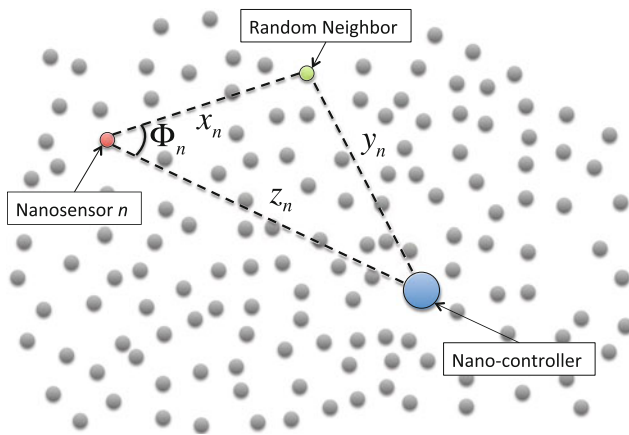


Fig. 2 Graphical representation of the nanosensor network for the computation of the probability of energy savings

probability of having a total average energy per bit consumption when adopting multi-hop transmission $E_{b\text{-multi-hop}}(n)$ which is lower than the average energy per bit consumption $E_{b\text{-direct}}(n)$ achieved with a direct path. This is expressed as follows:

$$P_{ES}(n) = \Pr\{E_{b\text{-multi-hop}}(n) \leq E_{b\text{-direct}}(n)\}. \quad (3)$$

The expression in (3) is translated into the probability of having at least one neighbor nanosensor, whose distance to the nano-controller is denoted as x_n , for which the energy per bit consumption when adopting multi-hop transmission is lower than the energy per bit consumption achieved with a direct path, as shown in Fig. 2. The energy per bit consumption when adopting multi-hop transmission with this neighbor nanosensor is equal to the sum of the energy per bit $E_{bit}(x_n)$ to transmit at a distance x_n , the energy per bit $E_{bit}(y_n)$ to transmit at a distance y_n between the neighbor and the nano-controller, and the energy E_r spent at the neighbor to receive one bit, which is a constant design parameter. The energy per bit consumption achieved with a direct path is equal to the energy per bit $E_{bit}(z_n)$ to transmit at a distance z_n between the nanosensor n and the nano-controller. As a consequence, the expression in (3) becomes

$$P_{ES}(n) = \Pr\{\exists(x_n, y_n) : E_{bit}(x_n) + E_{bit}(y_n) + E_r \leq E_{bit}(z_n)\}, \quad (4)$$

where x_n and y_n are the distance between the neighbor nanosensor and the nanosensor n , and the distance between the neighbor nanosensor and the nano-controller, respectively, as shown in Fig. 2. \exists denotes the existence of a node whose distances x_n and y_n satisfy the inequality in (4). z_n is the distance between the nano sensor n and the nano-controller, which is a known parameter to the nano-controller for each nanosensor n .

The probability $P_{ES}(n)$ of energy savings by multi-hop transmission for the nanosensor n is a function of the density ρ of nanosensors and the distance z_n between the nanosensor n and the nano-controller, while the distance x_n between the nano sensor n and a random neighbor and the distance y_n between the neighbor and the nano-controller are considered random variables which depend on a spatial Poisson counting process [12] whose rate is equal to the density ρ of nanosensors. As a consequence, the expression in (4) is equivalent to one minus the probability in aforementioned spatial Poisson process of having a count equal to zero in the area $S(z_n)$, derived from (1), and it is expressed as follows:

$$P_{ES}(n) = 1 - e^{-\rho S(z_n)}, \quad (5)$$

where $S(z_n)$ is defined as the area spanned by all the possible values for the coordinates of a neighbor nanosensor in the plane defined by $x_n \in [0, \infty]$ and $\Phi \in [0, 2\pi]$, which is the angle between the line connecting the nanosensor n and the nano-controller and the line connecting the nanosensor n and the neighbor, as shown in Fig. 2 which satisfy the inequality in (4). The area $S(z_n)$ is therefore computed through the following expression:

$$S(z_n) = \iint_{\{(x_n, \Phi) | E_{bit}(x_n) + \hat{E}_{bit}(x_n, \Phi) \leq E_{bit}(z_n) - E_r\}} x dx d\phi. \quad (6)$$

where $E_{bit}(x_n)$, $E_{bit}(z_n)$, and $\hat{E}_{bit}(x_n, \Phi)$ are the average energy per bit to transmit at a distance x_n , z_n , and from the neighbor nanosensor to the nano-controller, respectively, and guarantee a constant Signal-to-Noise Ratio SNR at a receiver. In the following, we detail the formulas for these parameters necessary to evaluate (6).

The average energy per bit $E_{bit}(l)$ to transmit at a distance l is defined as the ratio between the transmission power $P(l)$ spent at a nanosensor and the maximum transmission bit-rate $C(l)$, both functions of the distance l between the transmitting nanosensor and the receiver, which can be either another nanosensor or the nano-controller. This is expressed as follows:

$$E_{bit}(l) = \frac{P(l)}{C(l)}. \quad (7)$$

The transmission power $P(l)$ spent at a nanosensor as a function of the distance l is defined as the power necessary in transmission to guarantee a constant Signal-to-Noise Ratio SNR at a receiver placed at a distance l from the transmitting nanosensor. This is expressed as

$$P(l) = \int_{B_{3dB}(l)} \text{SNRA}(l, f) S_N(l, f) df, \quad (8)$$

where $A(l, f)$ and $S_N(l, f)$ are the total path loss and the total molecular absorption noise Power Spectral Density

(PSD) as a function of the distance l and the frequency f , and $B_{3dB}(l)$ is the 3dB bandwidth as a function of the distance l [8]. The total path loss $A(l, f)$ is computed through the following expression:

$$A(l, f) = \left(\frac{4\pi f_0 l}{c}\right)^2 e^{k(f)l}, \tag{9}$$

where c is the speed of light in the vacuum, $k(f)$ is the molecular absorption coefficient as a function of the frequency f , and f_0 is the design center frequency [18]. The total molecular absorption noise PSD S_N is contributed by the atmospheric noise S_{N_0} [2] and the induced noise S_{N_1} , and can be obtained as

$$S_N(l, f) = S_{N_0}(l, f) + S_{N_1}(l, f), \tag{10}$$

$$S_{N_0}(l, f) = \lim_{l \rightarrow \infty} k_B T_0 (1 - \exp(-k(f)l)) \left(\frac{c}{\sqrt{4\pi f_0}}\right)^2, \tag{11}$$

$$S_{N_1}(l, f) = S(f)(1 - \exp(-k(f)l)) \left(\frac{c}{4\pi f_0}\right)^2, \tag{12}$$

where l refers to the transmission distance, f stands for the frequency, k_B is the Boltzmann constant, T_0 is the room temperature, k is the molecular absorption coefficient, c is the speed of light in the vacuum, f_0 is the design center frequency, and S is the PSD of the transmitted signal. In this paper, we consider the following assumption:

- The frequency range defined by the 3dB bandwidth $B_{3dB}(l)$ as a function of the distance l is not affected by molecular absorption. This is expressed as follows:

$$k(f)|_{f \in B_{3dB}(l)} \approx 0, \tag{13}$$

As a consequence, the expressions of the total path loss and the total molecular absorption noise are simplified as follows:

$$A(l, f) = A(l) = \left(\frac{4\pi f_0 l}{c}\right)^2, \tag{14}$$

where l and f_0 are the distance and the design center frequency, respectively, and c is the speed of light in the vacuum;

$$S_N(l, f) = N_0, \tag{15}$$

where N_0 is a constant.

By taking into account that the transmission power $P(l)$ expressed in (8) guarantees a constant SNR at a receiver placed at a distance l from the transmitting nanosensor, the maximum transmission bit-rate $C(l)$ as a function of the distance l is expressed as follows:

$$C(l) = \int_{B_{3dB}(l)} \log_2(1 + \text{SNR}) df = B_{3dB}(l) \log_2(1 + \text{SNR}), \tag{16}$$

where $B_{3dB}(l)$ is the 3dB bandwidth as a function of the distance l [18].

The average energy per bit $E_{bit}(l)$ to transmit at a distance l is computed from (7), (8), (14), and (15), and (16), and it results in the following expression

$$E_{bit}(l) = \left(\frac{4\pi f_0}{c}\right)^2 \frac{N_0 \text{SNR}}{\log_2(1 + \text{SNR})} l^2, \tag{17}$$

where N_0 is a constant, l is the distance, f_0 is the design center frequency, c is the speed of light in the vacuum, and SNR is the constant signal-to-noise ratio guaranteed at the receiver.

The average energy per bit $\hat{E}_{bit}(x_n, \Phi)$ from the neighbor nanosensor to the nano-controller is computed by taking into account that the random variable y_n is a function of two independent random variables x_n and Φ , the distance between the nanosensor n and a neighbor, and the angle between the line that connects the nanosensor n with the nano-controller and the line that connects the nanosensor n with the neighbor, as shown in Fig. 2, through the law of cosines, expressed as

$$y_n = \sqrt{x_n^2 + z_n^2 - 2x_n z_n \cos \Phi}, \tag{18}$$

where z_n is the distance between the nanosensor n and the nano-controller, x_n is the distance between the nanosensor n and a random neighbor, y_n is the distance between the neighbor and the nano-controller, and Φ is the angle between the line connecting the nanosensor n and the nano-controller and the line connecting the nanosensor n and the neighbor. As a consequence, $\hat{E}_{bit}(x_n, \Phi)$ is expressed through the substitution of (18) into (17) as

$$\hat{E}_{bit}(x_n, \Phi) = \left(\frac{4\pi f_0}{c}\right)^2 \frac{N_0 \text{SNR}}{\log_2(1 + \text{SNR})} (x_n^2 + z_n^2 - 2x_n z_n \cos \Phi), \tag{19}$$

2.4 Critical neighborhood range for throughput-distance trade-off and infinite network lifetime

The Critical Neighborhood Range CNR is computed by investigating a trade-off for a nanosensor between the throughput and the distance from the receiving neighbor node that guarantees a predefined received SNR value, while at the same time satisfying the condition for infinite network lifetime.

The throughput $\Lambda(l)$ is defined as the maximum data rate at which a nanosensor can transmit at a distance l while guaranteeing a predefined received SNR value and infinite network lifetime. This is expressed as

$$\Lambda(l) = C(l) \lambda^c(l), \tag{20}$$

where $C(l)$ is the maximum transmission bit-rate as a function of the distance l , and $\lambda^c(l)$ is the Critical Transmission Ratio (CTR) given in [18], and defined as

the ratio between the energy harvesting rate λ_{harv} and the energy consumption rate $\lambda_{con}(l)$ for a nanosensor during transmission, expressed as

$$\lambda^c(l) = \frac{\lambda_{harv}}{\lambda_{con}(l)}, \tag{21}$$

where the energy harvesting rate λ_{harv} , when the nanosensors are provided by piezoelectric nano-generators to harvest vibrational energy [19], has the following expression [18]:

$$\lambda_{harv} = \frac{1}{2} C_{cap} V_g^2 \left(2 \frac{\Delta Q}{V_g C_{cap}} \exp\left(-\frac{\Delta Q}{V_g C_{cap}} n_{cycle}\right) - 2 \frac{\Delta Q}{V_g C_{cap}} \exp\left(-2 \frac{\Delta Q}{V_g C_{cap}} n_{cycle}\right) \right), \tag{22}$$

where V_g is the generator voltage, C_{cap} refers to the ultra-nano-capacitor capacitance, ΔQ is the electric charge harvested per cycle, and n_{cycle} is the rate of the vibrational energy source. The energy consumption rate $\lambda_{con}(l)$ is computed as the product between the maximum transmission bit-rate $C(l)$ and the average energy per bit $E_{bit}(l)$ to transmit at a distance l , expressed in (17), as

$$\lambda_{con}(l) = C(l)E_{bit}(l), \tag{23}$$

As a consequence, the throughput $\Lambda(l)$ that guarantees a predefined received SNR value and infinite network lifetime can be expressed after substituting (23) into (21) and (20) as

$$\Lambda(l) = \frac{\lambda_{harv}}{E_{bit}(l)}, \tag{24}$$

The CNR_n is defined as the distance between the nanosensor n and a potential neighbor for which the throughput $\Lambda(CNR_n)$ from the nanosensor n to the neighbor is on average equal to the throughput $\Lambda(y_n)$ from the neighbor to the nano-controller, where y_n is the distance

between the neighbor and the nano-controller. It is necessary to guarantee that the next hop neighbor is placed as close as possible to CNR_n in order to maximize the next hope distance range while at the same time achieving the highest possible throughput from the nanosensor n to the nano-controller. The CNR_n is computed through the following equation, whose main parameters are graphically represented in Fig. 3:

$$CNR_n = \left\{ x_n | x_n = \frac{\int_{(x_n, \Phi)} \sqrt{(z_n - x_n \cos \Phi)^2 + (x_n \sin \Phi)^2} d\Phi}{\int_{(x_n, \Phi)} d\Phi} \right\}, \tag{25}$$

subject to:

$$(x_n, \Phi) \in \{(x_n, \Phi) | E_{bit}(x_n) + \hat{E}_{bit}(x_n, \Phi) \leq E_{bit}(z_n) - E_r\}, \tag{26}$$

where the throughput $\Lambda(l)$ is computed through the expression in (24), (17), and (22), while x_n is the distance between the nanosensor n and a neighbor, Φ the angle between the line that connects the nanosensor n with the nano-controller and the line that connects the nanosensor n with the neighbor, z_n is the distance between the nanosensor n and the nano-controller, $E_{bit}(x_n)$ and $\hat{E}_{bit}(x_n, \Phi)$ are expressed in (17) and (19), respectively, and E_r is the energy spent at the neighbor to receive one bit, which is constant design parameter.

Finally, the nano-controller computes the RTP_n as the power that the nanosensor n should use to achieve a predefined value for the received SNR at a receiver placed at a distance equal to CNR_n . The RTP_n is computed through the following expression:

$$RTP_n = \int_{B_{3dB}(CNR_n)} SNRA(CNR_n, f) S_N(CNR_n, f) df, \tag{27}$$

where $A(l, f)$ and $S_N(l, f)$ are the total path loss and the total molecular absorption noise PSD computed for a value of the distance equal to CNR_n , and as a function of the frequency f , respectively, and $B_{3dB}(CNR_n)$ is the 3dB bandwidth for a distance CNR_n [18]. The total path loss $A(CNR_n, f)$ at a distance CNR_n is computed through the expression in (9), while the noise PSD $S_N(CNR_n, f)$ is given by (15).

2.5 Random back-off time for node load fairness

The availability to be the next hop for the nanosensor n is decided by a nanosensor m at time instant t upon starting the reception of the incoming data D_n from the nanosensor n transmitted in selected time slots of the MH sub-frame, as expressed through the block scheme in Fig. 4. The nanosensor

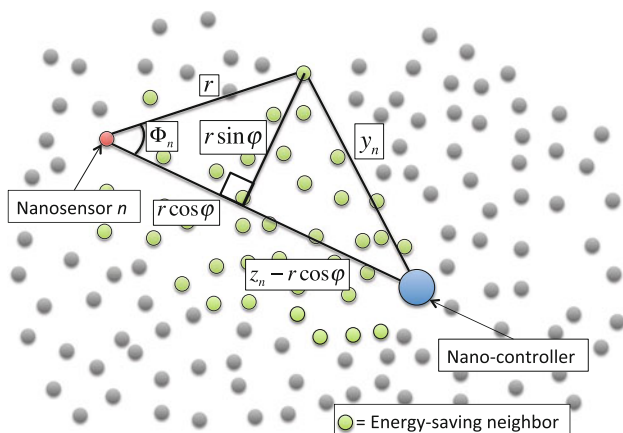


Fig. 3 Graphical representation of the main parameters involved in the computation of the CNR

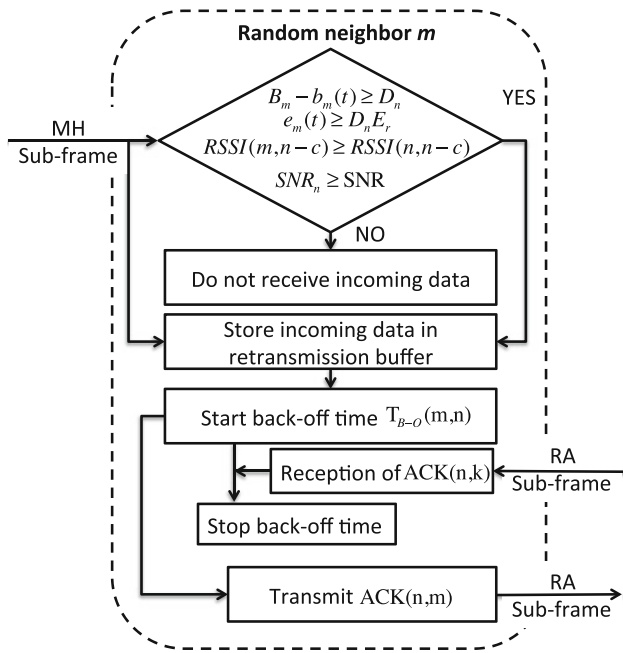


Fig. 4 Block Scheme of the algorithm executed at a random neighbor upon the reception of data from the nanosensor n in the MH sub-frame

m stores the received data in the retransmission buffer, sets the random back-off time $T_{B-O}(m)$, and it is available to be the next hop only if all the following conditions are met:

- There is enough room in the retransmission buffer of the nanosensor m to store the data received from the nanosensor n . This is expressed as follows:

$$B_m - b_m(t) \geq D_n, \tag{28}$$

where B_m is the total size in bits of the retransmission buffer of the nanosensor m , $b_m(t)$ is the size in bits of the data stored in the retransmission buffer of the nanosensor m at time t , and D_n is the size in bits of the incoming data from the nanosensor n , which is communicated to the nanosensor m by the nanosensor n at the beginning of the transmission.

- The energy $e_m(t)$ stored in the nanosensor m at time t is sufficient to complete the reception of the data from the nanosensor n . This is expressed as follows:

$$e_m(t) \geq D_n E_r, \tag{29}$$

where D_n is the size in bits of the incoming data from the nanosensor n , and E_r is the energy spent to receive one bit.

- The Signal-to-Noise Ratio SNR_n of the reception at the nanosensor m from the nanosensor n is higher than the constant SNR value guaranteed at the receiver defined in Sect. 2.2 This is expressed as

$$SNR_n \geq SNR, \tag{30}$$

- The nanosensor m is closer to the nano-controller than the nanosensor n . This translates into a condition based on

the Received Signal Strength Indicator (RSSI), which is a measurement proportional to the power received at a nanosensor. The condition states that the $RSSI(m, n - c)$ received at the nanosensor m upon a transmission from the nano-controller $n - c$, measured by the nanosensor m during any DL sub-frame, should be higher than the $RSSI(n, n - c)$ received at the nanosensor n upon a transmission from the nano-controller $n - c$, measured by the nanosensor n during any DL subframe and communicated to the nanosensor m before starting the transmission of the data in the MH sub-frame. This condition is expressed as follows:

$$RSSI(m, n - c) \geq RSSI(n, n - c), \tag{31}$$

If the aforementioned conditions are met, the nanosensor m stores in the retransmission buffer the data received from the nanosensor n , and starts the back-off time $T_{B-O}(m, n)$ upon the end of the data reception. The value of the back-off time $T_{B-O}(m, n)$ is a realization of an exponential distribution [12] expressed as follows:

$$f_{T_{B-O}(m,n)}(t) = \frac{e^{-\frac{t}{\hat{T}_{B-O}(m,n)}}}{\hat{T}_{B-O}(m,n)}, \tag{32}$$

where $\hat{T}_{B-O}(m, n)$ is the average value of the back-off time for the nanosensor m upon reception of data from the nanosensor n , and it is proportional to the $RSSI(m, n)$ received at the nanosensor m upon a transmission from the nanosensor n , expressed as follows:

$$\hat{T}_{B-O}(m, n) = K_{B-O} RSSI(m, n), \tag{33}$$

where K_{B-O} is a constant system design parameter. On the one hand, if during the back-off time the nanosensor m overhears an Acknowledgement $ACK(n, k)$ message in the RA sub-frame, where $k \neq m$, it stops the back-off time and deletes from the retransmission buffer the data received from the nanosensor n . On the other hand, upon timeout of the back-off time $T_{B-O}(m, n)$, the nanosensor m broadcasts an $ACK(n, m)$ in the RA sub-frame. The expression in (33) allows the nanosensors which are located farther from the nanosensor n , but closer to the CNR defined in Sect. 2.4, to have a shorter average back-off time than the other nanosensors, and consequently to be more likely selected as the next hop for the transmission of the data coming from the nanosensor n .

2.6 Optimal scheduling of the up link and multi hop sub-frames

2.6.1 Up link sub-frame scheduling

The UL sub-frame scheduling algorithm is required to schedule the transmissions of nanosensors which use direct/single-hop communications with the nano-controller.

In this case, based on Theorem 2 in [18], the nanosensors can be divided into two groups: **near-region sensors** and **far-region sensors**. The near-region sensors, which are within a distance D from the nano-controller, always have their energy harvesting rate λ_{harv} larger than their energy consumption rate $\lambda_{con}(l)$. This means that the maximum single-user throughput $\Lambda^{near}(l)$ of a near-region sensor can approach its maximum achievable data rate $C(l)$ defined in (16) as follows:

$$\Lambda^{near}(l) = C(l), \forall l < D. \quad (34)$$

In contrast to the near-region sensors, the far-region sensors, which are at least D far away from the nano-controller, always have their energy harvesting rate λ_{harv} less than their energy consumption rate $\lambda_{con}(l)$. Therefore, the far-region sensors always need to enter the sleep state for recharging before their next packet transmissions. This implies that the far-region sensors have the maximum single-user throughput $\Lambda^{far}(l)$ necessarily smaller than the maximum achievable data rate $C(l)$. This indicates the unbalanced transmission rates between near-region sensors and far-region sensors. Specifically, we have the following expression:

$$\Lambda^{far}(l) = \lambda^c(l)C(l), \forall l \geq D, \quad (35)$$

where CTR $\lambda^c(l)$ is always less than 1.

Based on the above observations, we adopt a similar scheduling as in [18], which decides on the packet transmission order of the nanosensors with the objective to guarantee the infinite network lifetime with balanced single-user throughput between far-region nanosensors and near-region nanosensors. The proposed scheduling algorithm involves the following steps.

Step 1: Calculate the minimum transmission period (MTP) per packet T_i for each nanosensor. Specifically, a near-region nanosensor has the following MTP:

$$T_i = N_{bits}/\Lambda^{near}(l_i), \quad (36)$$

and a far-region nanosensor has the following MTP:

$$T_i = N_{bits}/\Lambda^{far}(l_i). \quad (37)$$

Next, set the initial schedule length $L^\Gamma = \max_{i \leq M} T_i$, where M is the total number of nanosensors within the cluster. Let $l_{max} = \max_{i \leq M} l_i$. This results in

$$L^\Gamma = N_{bits}/\Lambda^{far}(l_{max}). \quad (38)$$

Step 2: Associate each nanosensor n_i with a schedule S_i . Set the packet counter in S_i as $N_i^\Gamma = 0$. Then, calculate the packet transmission time as follows:

$$T_i^{pk} = N_{bits}/R_{opt}(l_i) \quad (39)$$

for each nanosensor n_i . Next, arrange the nanosensors $\{n_i\}_{i \leq M}$ in the order of increasing maximum single-user

throughput Λ . Assign each nanosensor a priority $p_i = i$, i.e., the nanosensor with smaller Λ has higher priority.

Step 3: At the initial schedule decision time $\tau = 0$, the nanosensor n_i is scheduled to transmit at τ if the following three conditions are satisfied. (1) It has the highest priority. (2) The *backward difference* between the current time τ and the start time of n_i 's previous packet is not smaller than its MTP per packet T_i , i.e.,

$$\tau - s_{i,N_i^\Gamma} \geq T_i. \quad (40)$$

(3) The *forward difference* between the current time τ and n_i 's first packet transmission time is not smaller than its MTP per packet T_i . This is expressed as follows:

$$L^\Gamma - \tau + s_{i,1} \geq T_i. \quad (41)$$

If n_i is scheduled to transmit at time τ , the next schedule decision time follows $\tau = \tau + T_i^{pk}$.

Step 4: Repeat Step 3 until every nanosensor i is done sending the total amount of P_i packets, which is specified by a nanosensor i when it sends the request message to the nano-controller.

2.6.2 Multi-hop sub-frame scheduling

The MH sub-frame scheduling aims to schedule the transmission order for the nanosensors for which the nano-controller decided for a multi-hop transmission. We adopt the same scheduling algorithm as for the UL sub-frame case by redefining the near-region nanosensors and far-region nanosensors. More specifically, we define l_{ij} as the distance between a nanosensor i and relay node j . Then, the near-region nanosensors are characterized by a distance l_{ij} less than the critical distance D^c , defined as the distance that satisfies $\lambda_{D^c} = 1$. The far-region nanosensors are characterized by a distance l_{ij} larger than the critical distance D^c . Then, the maximum single-user throughput of the near-region and far-region nanosensors is computed through (34) and (35). Then, the scheduling algorithm as described for the UL sub-frame case is applied.

3 Numerical results

In this Section, we evaluate the performance of the proposed framework by means of extensive network simulations and discuss the results in detail. In Sect. 3.1, we describe the simulation setup and the applied parameter values, while in Sect. 3.2 we present the numerical results of the main quantities involved in the routing framework. Finally, in Sect. 3.2 we present an evaluation of the proposed routing framework against single-hop communication in terms of energy savings, capacity, and delay.

3.1 Simulation setup

In our simulation, we use the following parameter values. As shown in Fig. 5, the nanosensors are deployed according to a spatial homogeneous Poisson process as described in Sect. 2.1, where the density ρ has a value corresponding to a count of 100 nanosensors within an area S equal to a circle with radius 10 mm. The Terahertz Band channel is modeled as in [8], for a standard gaseous medium with 10% of water vapor molecules. The size of a packet is set to 256 bits, while the predefined value for the received SNR, on the basis of which we based the computation of the probability of energy savings in Sect. 2.3, the critical neighborhood range in Sect. 2.4, and the random neighbor algorithm in Sect. 2.5, is set to 10. The piezoelectric energy harvesting system has the following parameters. We consider a capacitor with $C_{cap} = 9\text{nF}$ charged at $V_g = 0.42\text{V}$ for the computation of the energy $e_m(t)$ stored in the nanosensor m at time t used in (29). For the computation of the energy harvesting rate λ_{harv} in (22), an ambient vibration with an average time between vibrations $t_{cycle} = 1/50\text{s}$ is considered. The amount of charge ΔQ harvested per cycle is 6 pC. The battery is fully discharged at the beginning of a simulation. The value of the energy E_r spent at a neighbor to receive one bit is set to 1/10 of the energy $E_{bit}(l)$ expressed in (17) required to transmit a bit at a distance l equal to 1 mm. The simulation of the whole WNSN is iterated 100 times, where each iteration accounts for different realizations of the stochastic process of the nano-controller decision for each nanosensor to go either for a multi-hop transmission or for a single-hop transmission, expressed in (2). The results in terms of energy, capacity and delay, presented in Sect. 3.3, are computed by averaging the values resulting from all the iterations. For

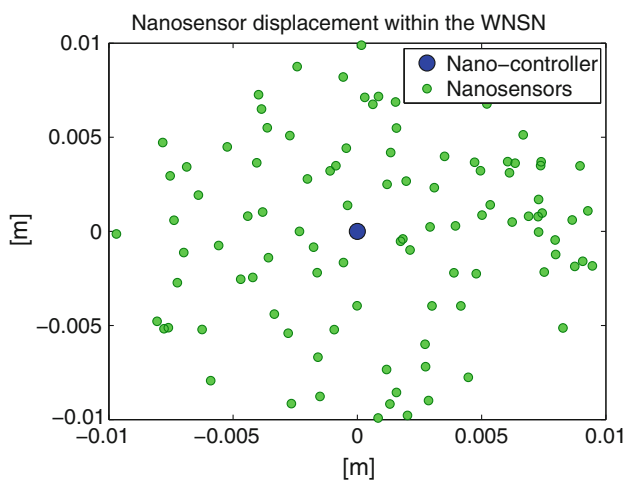


Fig. 5 Plot of the coordinates of 100 nanosensors deployed according to a homogeneous spatial Poisson process within a circle of radius 10 mm

computational reasons, the simulations of the multi-hop transmissions account only for a maximum of two hops between the source nanosensor and the nano-controller. As confirmed by the results presented in the following, this does not prevent from evaluating the overall benefits of having a multi-hop transmission in a WNSN.

3.2 WNSN routing framework

Numerical results for the area $S(z_n)$ defined as the area spanned by all the possible values for the coordinates of an energy-saving neighbor nanosensor in the plane defined by the distance and the angle from the source nanosensor are shown in Fig. 6, where the distance is limited between 0 and 10 mm, while the angle is limited between 0 and 2π rad. The area $S(z_n)$ is restricted to a region between -1.047 rad and 1.047 rad, and at a distance from the source nanosensor between 0.1 and 0.5 mm. This behavior is induced by the fact that the E_r spent at a neighbor to receive one bit is a constant value for all the possible neighbor nodes, and therefore is a constant term in the inequality in (4). As a consequence, the probability of energy savings is very low for both neighbors located too close to the source nanosensor, e.g., at less than 0.1 mm, and neighbors located too far from the source nanosensor, e.g., at more than 0.5 mm. The restriction of the area $S(z_n)$ within a limited range of angles is given by the fact that the energy savings have high values only for a neighbor located reasonably between the source nanosensor and the nano-controller. Any other neighbor would deviate the route of the packets from the source nanosensors too far away from the nano-controller.

Values for the probability $P_{ES}(n)$ of energy savings by multi-hop transmission are shown in Fig. 7, plotted for a distance of the source nanosensor from the nano-controller between 0.01 and 10 mm. As expected, the probability of energy savings has a low value for short distances, while it monotonically increases with the distance until reaching a value close to 1 for a distance longer than 8 mm. Clearly, as the distance of the source nanosensor from the nano-controller increases, the benefits of a multi-hop transmission in terms of energy saving become more and more evident.

3.3 Performance evaluation

The numerical values of the energy spent per nanosensor to transmit all its packets to the nano-controller is shown in Fig. 8, where the case of multi-hop routing, proposed in this paper, is compared to the case of single-hop communication. For short distances between a source nanosensor and the nano-controller, the energy spent is comparable, while as the distance gets longer, the energy saved through the multi-hop routing becomes higher and higher in agreement with the values of the probability of energy

Fig. 6 Area spanned by all the possible values for the coordinates of a neighbor nanosensor when the probability of energy saving is over a threshold

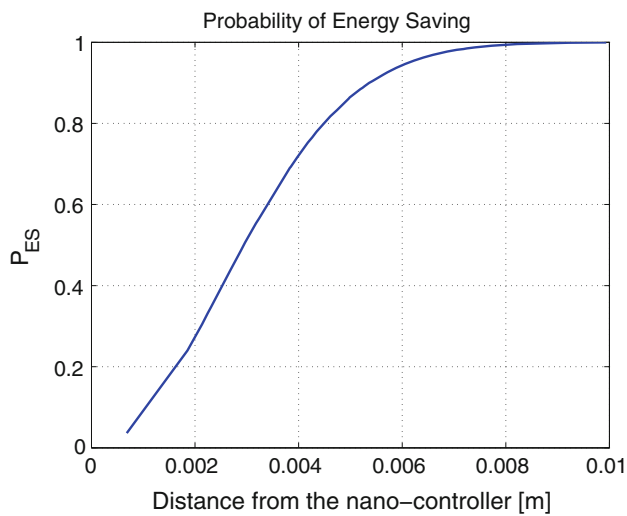
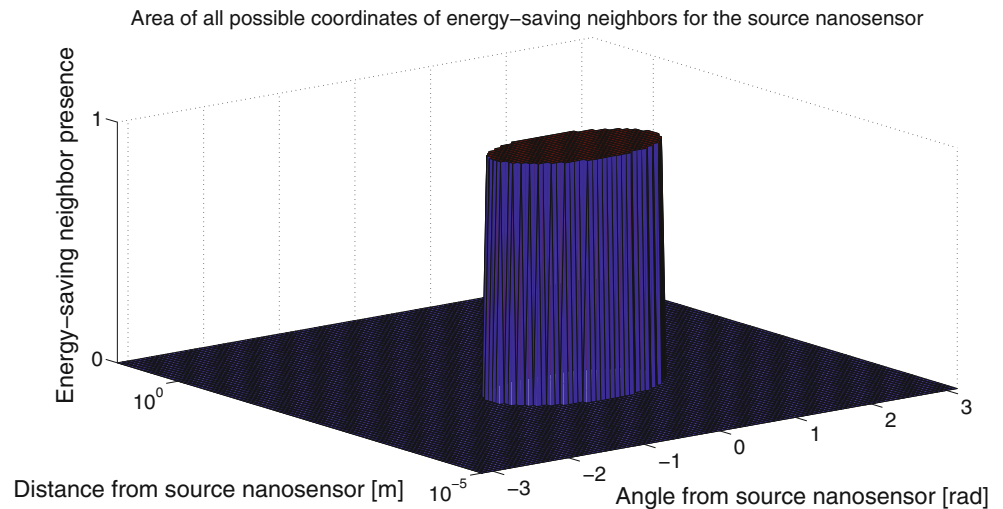


Fig. 7 Probability of energy saving by multi-hop for a distance between the source nanosensor and the nano-controller between 0.01 and 10 mm

savings shown in Fig. 7. These results confirm the benefits in terms of energy that can derive from the adoption of the proposed multi-hop routing framework in a WNSN.

The numerical results in terms of capacity in bits per channel use experienced by nanosensors at different distances from the nano-controller are shown in Fig. 9. At distances shorter than 0.3 mm, the capacity has the same value for both the cases, since the probability of energy saving by multi-hop, and consequently the probability of a multi-hop decision from the nano-controller, is very low. For a distance between 0.3 and 0.56 mm, the multi-hop transmission shows higher values for the capacity, while for a distance higher than 0.56 mm the benefits of the multi-hop transmission on the capacity are less evident. This behavior can be explained by the fact that in this simulation we account for a maximum of two hops between each source

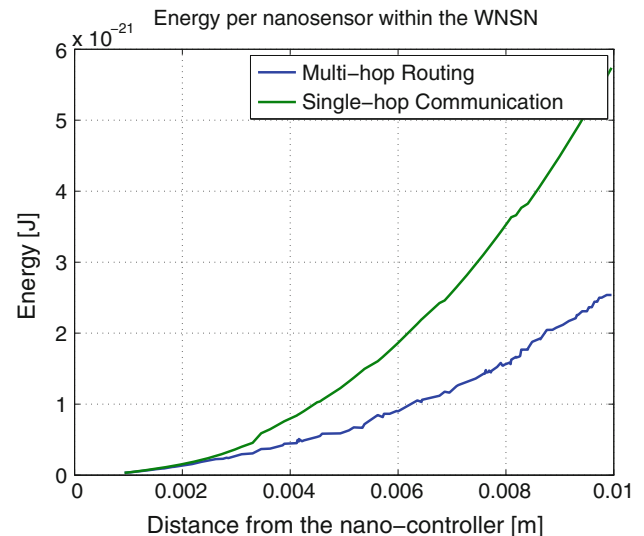


Fig. 8 Comparison between the energy spent per nanosensor for the case of multi-hop routing and for the case of single-hop communication. Each nanosensor is characterized by its distance from the nano-controller, ranging from 0.01 to 10 mm

nanosensor and the nano-controller. For this, we limit the number of hops even for a distance that would require a hop number, thus limiting the reachable capacity to a value comparable to the single-hop communication case.

Finally, the numerical results in terms of delay experienced by the packets transmitted by each source nanosensor to reach the nano-controller are shown in Fig. 10. For a distance between the source nanosensor and the nano-controller lower than 0.3 mm the delay has the same values for both the cases, since, as mentioned above, the probability of a multi-hop decision from the nano-controller is very low. For a distance between 0.3 and 0.82 mm, the multi-hop transmission is characterized by an overall lower delay if compared to the single-hop communication. This is

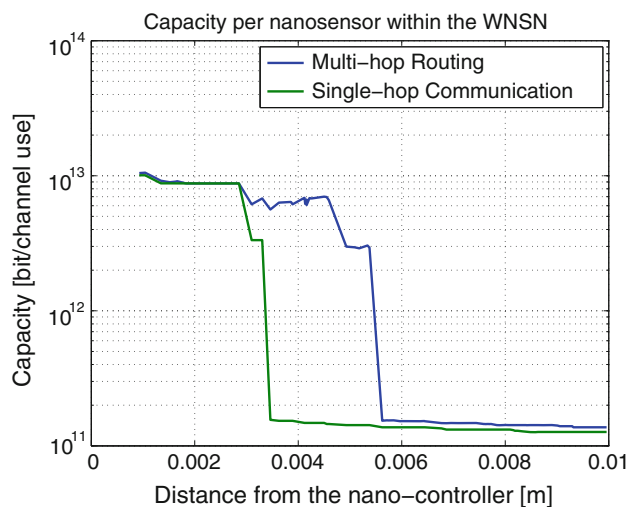


Fig. 9 Comparison between the capacity per nanosensor for the case of multi-hop routing and for the case of single-hop communication. Each nanosensor is characterized by its distance from the nano-controller, ranging from 0.01 to 10 mm

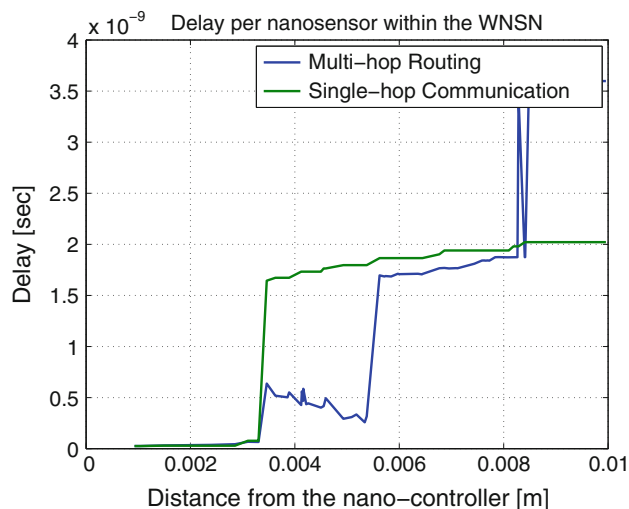


Fig. 10 Comparison between the delay per nanosensor for the case of multi-hop routing and for the case of single-hop communication. Each nanosensor is characterized by its distance from the nano-controller, ranging from 0.01 to 10 mm

explained by the increased throughput of the nanosensors when transmitting over shorter distances, to a neighbor, as opposed to a direct transmission to the nano-controller. Unfortunately, as the distance increases over 0.82 mm, the delay of the multi-hop transmission assumes much higher values than the values for the single-hop communication. This can be again explained by the fact that in this simulation we account for a maximum of two hops between each source nanosensor and the nano-controller. As a consequence, over 0.82 mm the benefits of a shorter transmission distance given by the multi-hop transmission are overtaken by the increased delay in the reception and

retransmission of packets at the next-hop neighbors with respect to the single-hop communication.

4 Conclusions

In this paper, we have proposed a routing framework for Wireless NanoSensor Networks (WNSNs) which takes into account the two main characteristics of the nanosensors, namely, their Terahertz Band wireless communication and their nanoscale energy harvesting process. Solutions from the literature, focused on energy-efficient routing Wireless Sensor Networks (WSN) with energy harvesting capabilities, are not directly applicable to WNSNs, since the peculiarities of the Terahertz Band communication, in particular the very unique distance-dependent behavior of the available bandwidth and the power control techniques that can be employed to reach the optimal transmission rate, are not taken into account. Moreover, other work focused on routing in WSN with energy harvesting nodes does not capture the particular characteristics of the energy harvesting processes at the nanoscale, in particular the collection of vibrational energy through piezoelectric nanogenerators. Based on the aforementioned nanosensor characteristics, combined with the nanosensors limitation in terms of computational resources, and the need to efficiently meet the conditions for perpetual network operations, the routing framework detailed in this paper is specifically designed to save the average energy harvested from the environment by the nanosensors, and at the same time increase the overall throughput in the transmission of information from the nanosensors to the nano-controller.

The routing framework proposed in this paper is designed on top of a previously proposed MAC protocol for the joint throughput and lifetime optimization in WNSNs, and it uses a hierarchical cluster-based architecture that pushes the network operation complexity towards the cluster heads, or nano-controllers. Moreover, this routing framework is based on the evaluation of the probability of saving energy through a multi-hop transmission, the tuning of the transmission power of each nanosensor for throughput and hop distance optimization, and the selection of the next hop nanosensor on the basis of their available energy and current load.

Numerical results are presented for the main quantities involved in the proposed routing framework, such as the probability of energy saving by performing multi-hop transmission from a source nanosensor as a function of its distance from the nano-controller. A performance evaluation of the proposed multi-hop routing framework is conducted through simulations, where key parameters such as the energy savings, the capacity, and the delay experienced by each nanosensor of the WNSN demonstrate the figures

of merit of the proposed framework over a more basic single-hop communication.

Acknowledgments The authors would like to thank Dr. Pu Wang and Dr. M. G. Abbas Malik for their invaluable support in the preparation of this paper. The material presented in this paper is based upon work funded by King Abdulaziz University, under Grant No. (11-15-1432/HiCi). The authors, therefore, acknowledge technical and financial support of KAU.

References

1. Akyildiz, I. F., & Jornet, J. M. (2010). Electromagnetic wireless nanosensor networks. *Nano Communication Networks (Elsevier) Journal*, 1(1), 3–19.
2. Box, F. (1986). Utilization of atmospheric transmission losses for interference-resistant communications. *IEEE Transactions on Communications*, 34(10), 1009–1015.
3. Cottone, F., Vocca, H., & Gammaitoni, L. (2009). Nonlinear energy harvesting. *Physical Review Letters*, 102(8), 080601. doi:10.1103/PhysRevLett.102.080601.
4. Deligeorgis, G., Coccetti, F., Konstantinidis, G., & Plana, R. (2012). Radio frequency signal detection by ballistic transport in y-shaped graphene nanoribbons. *Applied Physics Letters*, 101(1), 013502.
5. Drexler, K. E. (1986). *Molecular engineering: Assemblers and future space hardware*. Paper AAS-86-415, presented at Aerospace XXI, the 33rd annual meeting of the American Astronautical Society, Boulder, CO, 26–29 Oct 1986.
6. Drexler, E. (1992). *Nanosystems: Molecular machinery, manufacturing, and computation*. NY: Wiley.
7. Gammaitoni, L., Neri, I., & Vocca, H. (2009). Nonlinear oscillators for vibration energy harvesting. *Applied Physical Letters*, 94, 164102. doi:10.1063/1.3120279.
8. Jornet, J. M., & Akyildiz, I. F. (2011). Channel modeling and capacity analysis of electromagnetic wireless nanonetworks in the terahertz band. *IEEE Transactions on Wireless Communications*, 10(10), 3211–3221.
9. Jornet, J. M., & Akyildiz, I. F. (2012). Joint energy harvesting and communication analysis for perpetual wireless nanosensor networks in the terahertz band. *IEEE Transactions on Nanotechnology*, 11(3), 570–580.
10. Jornet, J. M., & Akyildiz, I. F. (2013). Graphene-based plasmonic nano-antenna for terahertz band communication in nanonetworks. To appear in *IEEE JSAC, Special Issue on Emerging Technologies for Communications*.
11. Otsuji, T., Boubanga Tombet, S., Satou, A., Ryzhii, M., & Ryzhii, V. (2013). Terahertz-wave generation using graphene—toward new types of terahertz lasers. *IEEE Journal of Selected Topics in Quantum Electronics*, 19(1), 8,400,209.
12. Papoulis, A., & Pillai, S. U. (2002). *Probability, random variables and stochastic processes*. McGraw-Hill.
13. Piesiewicz, R., Kleine-Ostmann, T., Krumbholz, N., Mittleman, D., Koch, m., Schoebel, J., & Kurner, T. (2007). Short-range ultra-broadband terahertz communications: Concepts and perspectives. *IEEE Antennas and Propagation Magazine*, 49(6), 24–39.
14. Ponomarenko, L. A., Schedin, F., Katsnelson, M. I., Yang, R., Hill, E. W., Novoselov, K. S., & Geim, A. K. (2008). Chaotic Dirac billiard in graphene quantum dots. *Science*, 320(5874), 356–358.
15. Sensale-Rodriguez, B., Yan, R., Kelly, M. M., Fang, T., Tahy, K., Hwang, W. S., Jena, D., Liu, L., & Xing, H. G. (2012). Broadband graphene terahertz modulators enabled by intraband transitions. *Nature Communications*, 3, 780.
16. Tamagnone, M., Gomez-Diaz, J. S., Mosig, J. R., & Perruisseau-Carrier, J. (2012). Reconfigurable terahertz plasmonic antenna concept using a graphene stack. *Applied Physics Letters*, 101(21), 214102.
17. Vicarelli, L., Vitiello, M.S., Coquillat, D., Lombardo, A., Ferrari, A.C., Knap, W., Polini, M., Pellegrini, V., & Tredicucci, A. (2012). Graphene field-effect transistors as room-temperature terahertz detectors. *Nature Materials*, 11, 865–871.
18. Wang, P., Jornet, J. M., Malik, M. A., Akkari, N., & Akyildiz, I. F. (2013). Energy and spectrum-aware MAC protocol for perpetual wireless nanosensor networks in the terahertz band. *Ad Hoc Networks (Elsevier) Journal*. (to appear)
19. Wang, Z. L. (2008). Towards self-powered nanosystems: From nanogenerators to nanopiezotronics. *Advanced Functional Materials*, 18(22), 3553–3567.

Author Biographies



Massimiliano Pierobon

received the Master of Science (B.S.+M.S.) degree in Telecommunication Engineering from the Politecnico di Milano, Milan, Italy, in 2005. He received the Ph.D. degree in Electrical and Computer Engineering from the Georgia Institute of Technology, Atlanta, GA, in August 2013. He is currently an Assistant Professor with the Department of Computer Science & Engineering at the University of Nebraska-Lincoln.

During 2006, Massimiliano Pierobon worked as a researcher in the R&D department of Siemens Carrier Networks, Milan, where he coauthored two filed patents on jitter buffer management. From January 2007 to July 2009 he was a graduate research assistant at the Politecnico di Milano in the fields of signal processing and pattern recognition. In November 2008 Massimiliano Pierobon joined the BWN lab, first as a visiting researcher and, from August 2009, as a Ph.D. student. He received the BWN Lab Researcher of the Year Award at the Georgia Institute of Technology for his outstanding research achievements in 2011. He is a member of IEEE, ACM, and ACS. His current research interests are in molecular communication theory for nanonetworks, communication engineering applied to intelligent drug delivery systems and biological circuit network engineering for microbial communication networks.



Josep Miquel Jornet

received the Engineering Degree in Telecommunication and the Master of Science in Information and Communication Technologies from the Universitat Politècnica de Catalunya, Barcelona, Spain, in 2008. He received the Ph.D. degree in Electrical and Computer Engineering from the Georgia Institute of Technology, Atlanta, GA, in 2013. He is currently an Assistant Professor with the Department of Electrical Engineering at the University at Buffalo, The State University of New York.

From September 2007 to December 2008, he was a visiting researcher at the Massachusetts Institute of Technology, Cambridge,

under the MIT Sea Grant program. He was the recipient of the Oscar P. Cleaver Award for outstanding graduate students in the School of Electrical and Computer Engineering, at the Georgia Institute of Technology in 2009. He also received the Broadband Wireless Networking Lab Researcher of the Year Award at Georgia Institute of Technology in 2010. He is a member of the IEEE and the ACM. His current research interests are in electromagnetic nanonetworks, graphene-enabled wireless communication, Terahertz Band communication networks and the Internet of Nano-Things.

Nadine Akkari received the B.S and the M.S. degrees in Computer Engineering from University of Balamand, Lebanon, in 1997 and 1999, respectively. She received the Master degree in Networks of Telecommunications from Saint Joseph University and the Faculty of Engineering of the Lebanese University, Lebanon, in 2001 and Ph.D. degree in Networking from National Superior School of Telecommunications (ENST), France, in 2006. She is currently an assistant professor with the faculty of Computing and Information Technology at King Abdulaziz University, Jeddah, Saudi Arabia. She is a member of IEEE. Her research interests are in wireless networks, mobility management protocols, and nanonetworks.



Suleiman Almasri was born in Amman, Jordan, in 1972. He received Diploma in Telecommunications Engineering in 1992 from Telecommunications College, Jordan, the B.Sc degree in Computer Science in 1998 from Philadelphia University, Jordan, MSc in Computer Science in 2005 from Amman Arab University, Jordan and PhD degree in Computer Science (Wireless and Mobile Networks) from Anglia Ruskin University, UK, in 2009. His

main research interests include

Technology, Mobile Networks, Mobile Information Systems, M-Learning, Location-Based Services, Communication Systems Applications and Database Systems.



Ian F. Akyildiz received the B.S., M.S., and Ph.D. degrees in Computer Engineering from the University of Erlangen-Nürnberg, Germany, in 1978, 1981 and 1984, respectively. Currently, he is the Ken Byers Chair Professor in Telecommunications with the School of Electrical and Computer Engineering, Georgia Institute of Technology, Atlanta, the Director of the Broadband Wireless Networking (BWN) Laboratory and the Chair of the Telecom-

munication Group at Georgia Tech. Since 2013, he is a FiDiPro Professor (Finland Distinguished Professor Program (FiDiPro) supported by the Academy of Finland) in the Department of Electronics and Communications Engineering, at Tampere University of Technology, Finland, and the founding director of NCC (Nano Communications Center). Since 2011, he is a Consulting Chair Professor at the Department of Information Technology, King Abdulaziz University (KAU) in Jeddah, Saudi Arabia. Since 2008, he is also an honorary professor with the School of Electrical Engineering at Universitat Politècnica de Catalunya (UPC) in Barcelona, Catalunya, Spain and the founding director of N3Cat (NaNoNetworking Center in Catalunya). He is the Editor-in-Chief of Computer Networks (Elsevier) Journal, and the founding Editor-in-Chief of the Ad Hoc Networks (Elsevier) Journal, the Physical Communication (Elsevier) Journal and the Nano Communication Networks (Elsevier) Journal. He is an IEEE Fellow (1996) and an ACM Fellow (1997). He received numerous awards from IEEE and ACM. His current research interests are in nanonetworks, Long Term Evolution Advanced (LTE-A) networks, cognitive radio networks and wireless sensor networks.